URSI RCRS 2024, Nainital, India, 22 - 25 October, 2024

Compact dual-mode microstrip bandpass filter with spurious harmonics suppression

Tarun K. Das[(1)], Niloy Mondal[(2)], Asmita Bhattacharya[(3)] and Sayan Chatterjee[(4)]
(1) Dept. of ECE, Future Institute of Engineering and Management, Kolkata, India
(2, 3, 4) Dept. of ETCE, Jadavpur University, Kolkata, India

Abstract

Present article proposes a compact microstrip dual-mode square loop resonator bandpass filter designed for the wireless communication system. The proposed filter operates at a center frequency of 2.5 GHz and has a bandwidth of 0.12 GHz (fractional bandwidth of 4.8%). The conventional dual-mode filter suffers from the presence of the spurious harmonics although it exhibits enhanced skirt characteristics in the passband. Accordingly, the input and output feed ports of the conventional filter have been cascaded with a folded one-section band-stop filter. One quarter-wavelength resonator and one segment of anti-coupled lines with short circuits at one end have been used to make such bandstop filter to generate selective transmission zeros in the stopband. As a result, an extended stopband upto $4f_0$ (f_0 is the center frequency) with a rejection level more than 32 dB has been obtained in simulation. Additionally, improved skirt characteristics have been exhibited by the generation of two sharp transmission zeros with attenuation levels more than 45 dB.

1. Introduction

Wireless communication systems are developing at a rapid rate, making small, lightweight, affordable, and highly effective radio frequency (RF) equipment. Bandpass filters (BPFs), a crucial passive part of the RF circuitry, are gaining a lot of attention from researchers due to their small size and extremely selective design. A superior BPF design will be achieved by obtaining a low insertion loss in the passband and good suppression in the out-of-band area. In this context, microstrip dual-mode resonator bandpass filters play an important role due to their ability to provide compact size, achieve high selectivity and improved passband performance due to the dual-mode operation, lower insertion loss due to the high quality factor providing narrow passband bandwidth, and flexibility in design [1]. The most attractive feature of the dual-mode filters is the creation of transmission zeros (TZs) on both sides of the passband, increasing selectivity and suppressing the out-of-band region. Compact planar microstrip BPFs with dual-mode architecture and a range of resonator types have been developed extensively in recent years in response to application requirements in microwave and radio frequency systems [2-4]. By linking the two degenerate modes with perturbation along the orthogonal plane of resonators, such dual-mode filters can be built. Numerous dual-mode planar resonator configurations including loop [2], patch [3], and fractal structures [4], have been documented in the literature for the purpose of designing BPFs with good selectivity and compact size. For instance, Sierpinski–Knopp fractal geometry has been employed in [4] to achieve a compact filter size of 24.6×24.6 mm^2. However, for all such filters of [2-4] the primary objective is to improve the passband performance and achieve compactness by employing different types of perturbations. The effects of such perturbations on the harmonics' attenuation levels are not addressed. Thus, it may provide restrictions for such filters to be used for such applications like mixers and frequency synthesizers where existence of harmonics becomes a severe problem.

Accordingly, both the compactness and harmonics suppression have been studied in [5-8] by using different reactive elements. For instance, a very compact filter with size 5.98 mm × 5.66 mm has been proposed in [5] based on a 2-layer low temperature cofired ceramic (LTCC) substrate with a square resonator and two pairs of open-stubs in cascade. As a result, a wide stopband upto $3f_0$ with a rejection level of 21 dB has been obtained. Subsequently, in [6], half-mode substrate-integrated rectangular cavity has been employed to achieve a wide stopband upto $4.36f_0$ with a rejection level of 20 dB and compact size of $0.028\lambda_g^2$ (λ_g is the guided wavelength at f_0). Later, in [7], a wide stopband with a rejection level of 30 dB has been reported by cascading dual-mode fan-shaped patch resonator and single-mode uniform impedance resonators. However, the size of the filter is little large ($0.90\lambda_g \times 0.75\lambda_g$). For all such filters the rejection levels of the stopband have been limited to 30 dB.

In the present article, a single square loop dual-mode bandpass filter with center frequency of 2.5 GHz and fractional bandwidth of 4.8% has been proposed. A folded one-section bandstop filter has been cascaded with the input and output ports of the filter to suppress the spurious harmonics. A wide stopband upto $4f_0$ with a rejection level more than 32 dB has been achieved in simulation. The overall footprint area of the filter is $0.47\lambda_g \times 0.45\lambda_g$. The filters have been designed on FR4 substrate having a dielectric constant of 4.4, loss tangent of 0.02, and thickness of 1.6 mm.

2. Design of Dual-Mode Resonator Filter

The dual-mode is composed of two degenerate modes orthogonal to each other or splitting resonant frequencies that may be excited by perturbing stubs, notches, or asymmetrical feed lines [9, Ch. 11, pg. 404-410]. The perturbation is provided for square loop dual-mode resonator by a small patch at a 45° offset from its two orthogonal modes. Figure 1(a) shows the structure of a conventional dual-mode resonator bandpass filter.

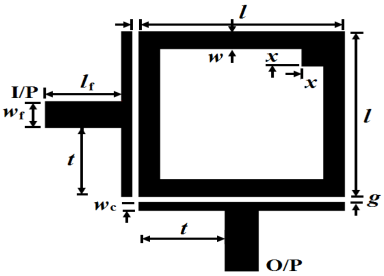

Figure 1. Layout of the conventional square-loop dual-mode resonator bandpass filter.

Based on the design specifications of the filter and by following the conventional transmission line theory [9], the dimensions of the filters have been computed and adjusted optimally in EM simulation (IE3D simulator) as l = 19.2 mm (λ_g/4), w = 2 mm, g = 0.3 mm, x = 2.4 mm, w_c = 1 mm, and t = 8.16 mm. The value of l_f = 5 mm and w_f = 3.06 mm have been computed for 50 ohm feed port impedance for FR4 substrate. Figure 2(a) illustrates the comparison of $|S_{21}|$ (dB) plots between the single-mode and the dual-mode resonator with perturbation size x = 2 mm. It has been observed that very poor selectivity has been achieved for single-mode configuration with Chebyshev characteristics, whereas the selectivity has been enhanced greatly for dual-mode configuration exhibiting quasi-elliptic characteristics by the generation two sharp transmission zeros f_{z1} and f_{z2}. Accordingly, Figure 2(b) demonstrates the influence of the variation of the perturbation size x on $|S_{21}|$ (dB) response of the dual-mode filter. It has been revealed that the resonant mode is split into two modes with the incremental value of x.

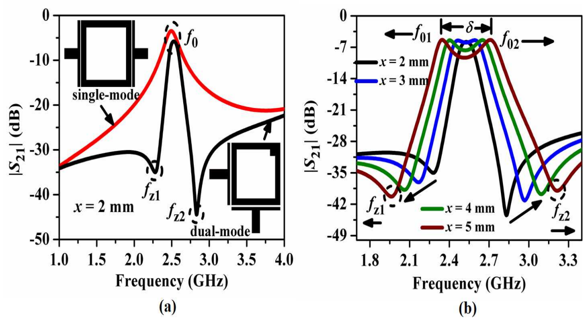

Figure 2. (a) Comparison of $|S_{21}|$ plots between single-mode and dual-mode structure, (b) effect of change of x (mm) on $|S_{21}|$ (dB) variations.

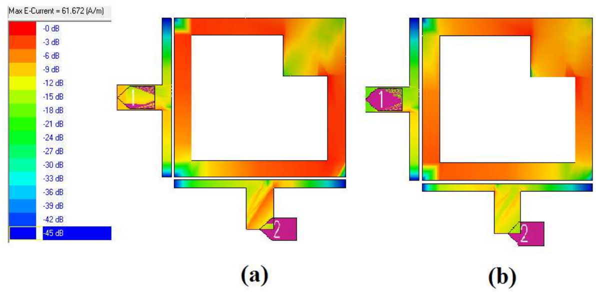

Figure 3. Surface current distribution for dual-mode filter at f_{01}= 2.35 GHz (mode-I), and at f_{01} = 2.71 GHz (mode-2) for x = 5mm.

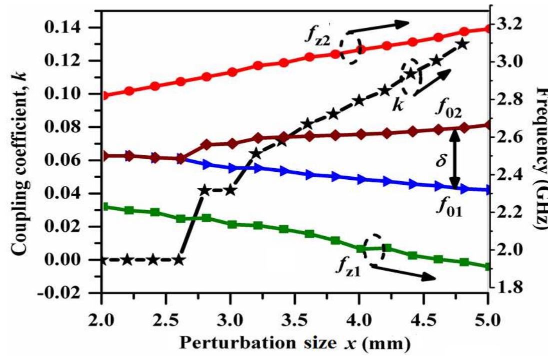

Figure 4. Dual-mode split characteristics for variations in perturbation length x.

The lower resonant frequency f_{01} corresponding to mode-I shifts to lower frequency region, whereas the upper resonant frequency f_{02} corresponding to mode-II shifts to higher frequency region as the perturbation size increases. In addition, the lower transmission zero f_{z1} shifts toward the lower frequency with decrease in the attenuation level, whereas the upper transmission zero f_{z2} shifts toward the higher frequency with increase in the attenuation level. The surface current distribution at mode f_{01}= 2.35 GHz (mode-I), and at f_{01} = 2.71 GHz (mode-2) for x = 5 mm is elaborated in Fig. 3(a)-(b). It has been revealed that the strength of the surface current is quite large at the two degenerate modes reaching the output port. Accordingly, the dual-mode splitting characteristics and the coupling coefficient variation with the incremental values of perturbation size x (mm) are illustrated in Fig. 4. As the perturbation sixe x increases from 2 mm to 5 mm, the two degenerate modes split after x = 2.7 mm and the difference between the two resonant frequency $\delta = f_{02}$-f_{01} gradually becomes wide. As a result, the bandwidth of the passband of the filter increases. It justifies the fact the proper value of the perturbation size is utmost important for the perfect coupling between two degenerate modes. Thus, the optimum value of the perturbation size has been selected as 2.4 mm for the absolute coupling between the degenerate modes at f_0 = 2.5 GHz. The variation of f_{z1} and f_{z2} are also significant as depicted in Fig. 4 for achieving narrow bandwidth and improvement of the skirt characteristics of the passband. After performing all parametric studies for g, t and w_c (refer Fig. 1), the final dual-mode single square-loop bandpass filter has been designed with a size of 25.5 mm × 25.5 mm i.e.,

$0.37\lambda_g \times 0.37\lambda_g$ including the feed ports. Figure 5 illustrates the simulated *S*-parameters plots for the filter. It has been observed that two sharp transmission zeros f_{z1} and f_{z2} have been generated at the passband edges at 2.2 GHz and 2.9 GHz with attenuation levels more than 41 dB. An insertion loss of 1.1 dB and return loss more than 20 dB have been obtained in the passband as highlighted in the inset diagram. It can be concluded that the conventional dual-mode filter has exhibited improved passband performance. However, the presence of second harmonic at 5 GHz and third harmonic at 7.5 GHz with large attenuation levels of 5 dB and 8 dB respectively, restrict the applications of the dual-mode filter. Subsequently, the suppression mechanism of such harmonics by cascading the folded bandstop filter has been studied in the next section.

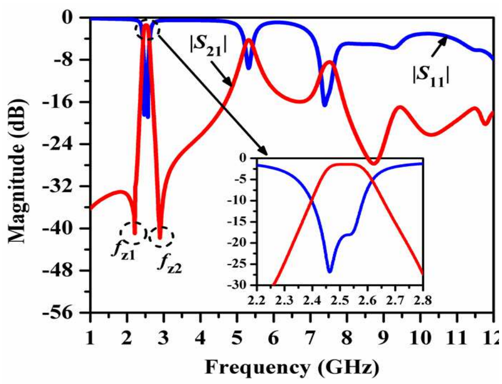

Figure 5. EM simulated *S*-parameters plots for a square-loop dual-mode bandpass filter.

3. Design of Folded Bandstop Filter (BSF)

Figure 6 illustrates the layout of the folded BSF structure as proposed in [10]. The BSF is the cascade combination of a single open-circuited quarter-wavelength resonator (l_c, g_c, and w_c) and one section of quarter-wavelength frequency-selecting coupling structure (FSCS) (l_r and w_r). FCFS is basically quarter-wavelength long at f_0 of the required stopband. Due to the inhomogeneous nature of the microstrip structure, there always exists a phase velocity imbalance between the even-and odd-mode of the propagating signal. By adjusting the coupling length l_c such phase velocity imbalance can be compensated and transmission zeros can be generated at selective locations in the stopband of the BSF.

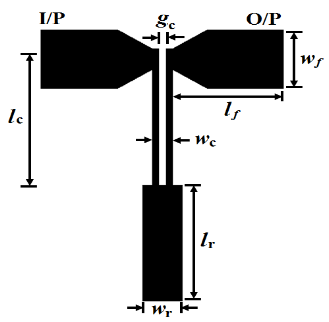

Figure 6. Layout of the bandstop filter [10].

For the present work, the primary objective for using the BSF to generate the transmission zeros in the stopband of the conventional dual-mode filter after 3.5 GHz onwards such that a wide stopband can be obtained with a high rejection level (more than 30 dB). For simplicity, the center of the stopband (3.5 GHz to 15 GHz) is calculated as 9.25 GHz and the length of l_r and l_c have been considered as quarter wavelength at 9.25 GHz. Accordingly, after performing various parametric studies for the BSF structure and after fine tuning in simulation, the optimum dimensions of the BSF have been selected as l_r = 4. 6 mm, w_r = 2.51 mm, l_c = 5.56 mm, w_c = 0. 2 mm, g_c = 0.2 mm, l_f = 5 mm, and w_f = 3.06 mm. The wideband *S*-parameters plots of the BSF are depicted in Fig. 7. It has been observed that two sharp transmission zeros f_{zs1} and f_{zs2} have been generated at 5.05 GHz and 12.7 GHz with attenuation levels of 31 dB and 35 dB respectively. Moreover, an attenuation level more than 12 dB has been maintained from 4 GHz to 15 GHz. Such bandstop performance of BSF has been utilized for the conventional dual-mode filter to suppress the spurious harmonics as discussed in the next section.

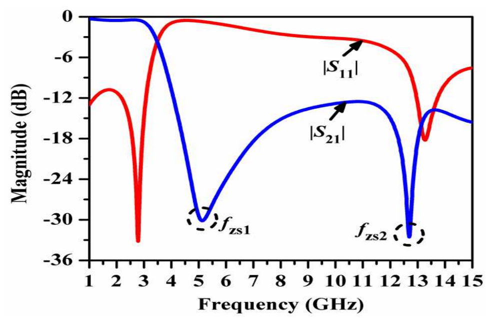

Figure 7. Simulated *S*-parameters plots for the BSF.

4. Harmonics Suppression for the Dual-Mode Filter with BSF

Figure 8 demonstrates the layout of the dual-mode filter with BSFs cascaded with the feed ports. The overall circuit area of the filter becomes 32.4 mm × 31.1 mm, i.e., $0.47\lambda_g \times 0.45\lambda_g$. Accordingly, Fig. 9(a)-(b) illustrate the comparison of the simulated $|S_{21}|$ and $|S_{11}|$ plots respectively. It has been observed from Fig. 9(a) that the passband insertion loss becomes less than 1.12 dB. The skirt characteristics of the final filter have been enhanced greatly due to the generation of two sharp transmission zeros at the passband edges with attenuation levels more than 45 dB.

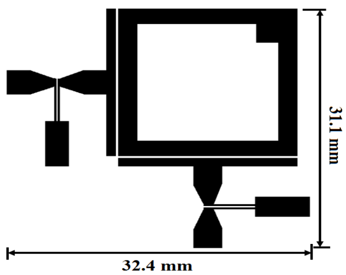

Figure 8. Layout of the final dual-mode filter with BSF.

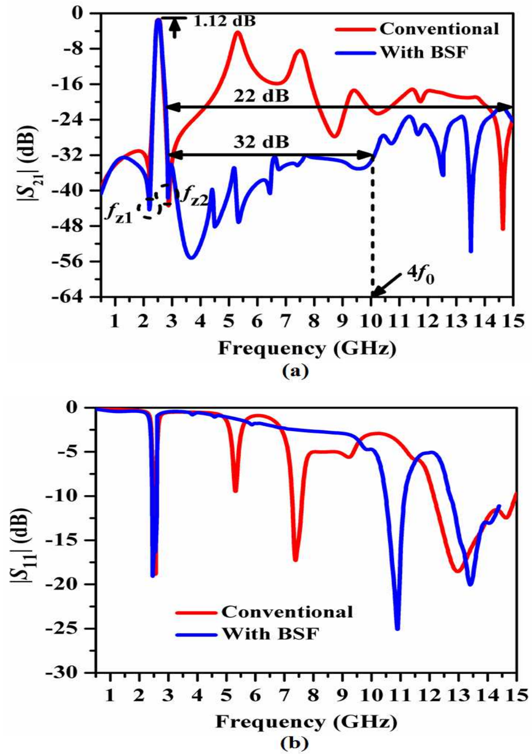

Figure 9. Comparison of the *S*-parameters plots.

In addition, a wide stopband upto $4f_0$ with a rejection level more than 32 dB and upto $6f_0$ with a rejection level more than 22 dB have been obtained. The return loss becomes more than 18 dB as obtained from Fig. 9(b). Table 1 compares the results obtained in the proposed work with similar published works. Here, δf = fractional bandwidth (%), *IL* = insertion loss in dB, *RL* = return loss in dB, *SBW* = stopband bandwidth in GHz, *SBRL* = stopband rejection level in dB. It has been observed that proposed work exhibits more stopband bandwidth than [6, 9] with more rejection level than [6, 8, 9, 10].

Table 1 Comparison of similar published works.

Ref.	f_0 (GHz)	δf (%)	*IL/RL* (dB)	*SBW* ($\times f_0$)	*SBRL* (dB)
6	3.55	14	1.1/16.	3	21
8	0.835	15.8	0.4/27	4.26	20
9	4.73	13	1.6/16	1.7	30
10	2.45	3.4	1.3/20	4.9	30
This	2.5	4.8	1.1/18	4	32

4. Conclusion

Present article describes the design a dual-mode square-loop bandpass filter centered at 2.5 GHz with a fractional bandwidth of 4.8%, with harmonics suppression performance. A combination of a pair of parallel-coupled lines and an open-circuited stub has been used to design the bandstop filter to be cascaded with the conventional dual-mode filter. As a result, a wide stopband upto $4f_0$ with a rejection level of 32 dB and upto $6f_0$ with a rejection level more than 22 dB has been achieved along with satisfactory passband performance in terms of insertion loss, return loss and skirt characteristics. The proposed filter is applicable for WLAN system.

7. References

1. J. Liu, F. Seyfert and K. -L. Wu, “Trapezoid Topology for Dual-Mode Bandpass Filters,” *IEEE Transactions on Microwave Theory and Techniques*, **72**, 7, pp. 4210-4217, July 2024, doi: 10.1109/TMTT.2023.3335929.

2. K. Song, Y. Zhu, M. Zhao, M. Fan, and Y. Fan, “Miniaturized bandpass filter using dual-mode hexagonal loop resonator”, *International Journal of Microwave and Wireless Technologies*, **9**, 5, pp. 1003-1008, June 2017, doi: 10.1017/S1759078716001094.

3. F. L. Zhao, M. H. Weng, C.Y. Tsai, R.Y. Yang, H.Z. Lai, and S.K. Liu, “A miniaturized high selectivity bandpass filter using a dual-mode patch resonator with two pairs of slots”, *Microwave and Optical Technology Letters*, **62**, 3, pp. 1145-1151, March 2020, doi: 10.1002/mop.32165.

4. S. Karthie, and S. L. Manibala, “Novel fractal-based dual-mode quasi-elliptic microstrip band-pass filter for WLAN applications,” *Applied Physics A*, **129**, 3, pp. 199, February 2023, doi:10.1007/s00339-023-06495-3

5. C. Li, L. Qian, Z. Zhang, Y. Wang, and B. Zhou, “Compact LTCC Dual-Mode Filter with Non-Orthogonal Feeding and Harmonics Suppression for 5G Applications,” *Progress In Electromagnetics Research Letters*, **92**, pp. 17-24, June 2020. doi:10.2528/PIERL20022705

6. R. K. Barik, S. Koziel, and A. Pietrenko-Dabrowska, “Broad stopband, low-loss, and ultra-compact dual-mode bandpass filter based on HMSIRC,” *Electronics*, **12**, 13, pp. 2831, June 2023, doi:10.3390/electronics12132831

7. C. Fan, K. Gong, B. Liu, Y. Liu, and Q. Liu, “Highly-selective microstrip bandpass filters based on new dual-mode fan-shape patch resonators,” *IET Microwaves, Antennas & Propagation*, **17,** pp. 797-806, August 2023, doi:10.1049/mia2.12395

8. S. Fu, C. Lian, Z. Xu, and Z. Wang, “Design of highly selective balanced bandpass filter with wide differential-mode stopband and high common-mode suppression,” *AEU-International Journal of Electronics and Communications*, **178**, pp. 155262, May 2024.

9. J. S. Hong, and M. J. Lancaster. *Microstrip Filters for RF/Microw Applications*. New York: Wiley; 2001.

10. M.-Y. Hsieh, and S.-M. Wang, “Compact and Wideband Microstrip Bandstop Filter”, *IEEE Microwave And Wireless Components Letters*, **15**, 7, pp. 472-474, July 2005, doi:10.1109/LMWC.2005.851572